Supporting Information

**Spontaneous Formation of CdSe Photoluminescent Nanotubes with Visible-light Photocatalytic Performance**

*Xiaopeng Huang, Virendra K. Parashar, and Martin A.M. Gijs**

# Tables of Contents

## Methods

**Materials.** Cadmium acetate hydrate ($Cd(Ac)_2 \cdot 2H_2O$, 99.9% purity), cadmium oxide (CdO), 1-octadecene (ODE), oleic acid (OAc), dioctylamine (97% purity, DOA), octylamine (99% purity, OAm), trioctylamine (98% purity, TOA), oleylamine (>98% purity, OLA), thioacetamide (TAA), trioctyl phosphine (TOP, 97% purity), selenium powder (Se), methanol, hexane, ethanol and dichloromethane were purchased from Sigma-Aldrich. All chemicals were used without further purification.

**Synthesis of CdSe NTs and 2D CdSe NCs.** A schematic drawing showing the synthesis procedures is shown in Figure S1. Before the synthesis of the CdSe NTs, the Cd precursor solutions were prepared in advance, as follows. 333 mg (1.25 mmol) of $Cd(Ac)_2 \cdot 2H_2O$ were sonicated in 1.5 mL (5 mmol) of DOA (a molar ratio of 1:4 between Cd and DOA was taken), followed by heating at 200 °C for 10 minutes to fully remove the water and get clear solution, which was labeled as "$Cd(Ac)_2$-DOA solution". For a typical CdSe NTs synthesis, 7.9 mg of Se powder was first dissolved (partly dispersed) in 3.6 mL of ODE and stirred at 260 °C for 10 min, after which 0.3 mL of $Cd(Ac)_2$-DOA Solution (a molar ratio of 2.5:1 between Cd and Se) was quickly injected. The solution rapidly turned turbid, followed by a change in color from white into yellow, and finally into a brown solution. After a given time (e. g. 8 min), the reaction was stopped by removal of the heater and the mixture was cooled down in air. Tubular CdSe NCs were produced mainly in the form of aggregates, together with some quantum dots as byproducts. For the purification, the cooled solution was mixed with a solution containing hexane and TOP (3:1, v/v) and centrifuged at a speed of 3000 rpm for 3 min. TOP was used to remove the unreacted Se precursor. The resulting supernatant was discarded, while the precipitates, mainly containing CdSe NTs, were collected and washed in hexane-TOP solution for two more times for 5 min. Afterwards, the collected products were twice washed in methanol by a dispersion and centrifugation process to remove the unreacted Cd precursor. Finally, the precipitates were dispersed in hexane for further characterization. Other 2D CdSe NCs such as nanoplatelets and curved nanosheets were prepared through similar

procedures by changing the reaction temperature and time. It is worth mentioning that, different from the classical hot injection method used for CdSe quantum dots preparation,[1] neither degassing the reactant before the reaction nor creating an inert atmosphere for the reaction is needed.

**Surface ligand exchange with oleic acid on 2D CdSe NCs.** First, the purified 2D CdSe NCs in hexane were centrifuged. After discarding the supernatant, the precipitate containing the 2D NCs was dispersed in 2 mL of a solution containing ODE and oleic acid (8:2, v/v). Then the solution was stirred at 200 °C for 10 min with a speed of 800 rpm. After cooling to room temperature, the resulting solution was purified in hexane for further characterization by centrifugation and redispersion.

**Control experiments to investigate the role of acetate and amine in CdSe NTs synthesis.** Control experiments were designed and performed in the absence of DOA or/and ODE; obtained reaction products are shown in Figure S9. In case of synthesis using DOA in the absence of ODE (Fig. S9b), 7.9 mg of Se powder was stirred in 3.6 mL of DOA at 260 °C to get the Se-DOA solution. Afterwards, 0.3 mL of $Cd(Ac)_2$-DOA (a molar ratio of 2.5:1 between Cd and Se) was quickly injected into the Se precursor solution and the reaction was kept going for 8 min. In case of synthesis using ODE in the absence of DOA (Fig. S9c-e), 15.8 mg of Se were mixed with 266 mg of $Cd(Ac)_2 \cdot 2H_2O$, and then ground into powder of homogenous color with a mortar and pestle. Then, 140.9 mg of the mixture were rapidly injected into a 3.6 mL ODE solution which was already heated to 260 °C. The reaction was kept for a variable time, like 8 min (Figure S9c), 16 min (Figure S9d) and 32 min (Figure S9e). For all control experiments, a further purification by repeating the centrifugation and redispersion of the precipitates in hexane three times was required. In case of synthesis without using DOA and ODE, 140.9 mg of the $Cd(Ac)_2 \cdot 2H_2O$-Se mixture, as prepared in the last step were heated for 8 min at 260 °C on a glass substrate. After that, the product was collected in a vial and dispersed in hexane for further characterization. In addition, to obtain the $Cd(Ac)_2$-DOA precipitates for further characterization, 0.3 mL of $Cd(Ac)_2$-DOA solution was quickly injected into 3.2 mL of ODE solvent at 200 °C at a stirring speed of 800 rpm. After 5 min, the white

precipitate was collected by centrifugation and washed twice in hexane by repeating the dispersion and centrifugation process. To investigate the influence of other alkylamines, $Cd(Ac)_2$-OAm, $Cd(Ac)_2$-TOA and $Cd(Ac)_2$-OLA precursors were first prepared by adding 333 mg (1.25 mmol) of $Cd(Ac)_2 \cdot 2H_2O$ into the corresponding amines at a molar ratio of 1:4 between Cd and amines, followed by heating at 200 °C for 10 minutes to fully remove the water. The synthesis of CdSe NCs using these $Cd(Ac)_2$-amine precursors was performed, in which the protocol was similar to that for CdSe NTs synthesis using $Cd(Ac)_2$-DOA at 260 ˚C for a reaction time of 8 min.

**Growth of a CdS shell to unfold the CdSe NTs.** The growth of a CdS shell using thioacetamide (TAA) and $Cd(oleate)_2$ was performed using the method reported by B, Dubertret et al[2]. Typically, 20 mg of TAA dissolved in 200 μL of OAm were added into 10 mg of purified CdSe NTs dissolved in 2 mL of dichloromethane. After a stirring mixing at 800 rpm for 10 min, 200 μL of the solution was fetched for further characterization (as shown in Figure S21). 200 μL of $Cd(oleate)_2$ dissolved in the OAm (0.1 M) was then added to the remaining solution and the stirring was stopped after a reaction time of 3 h (corresponding to the sample as shown in Figure S20). The purification of these samples was performed by repeating the dispersion and centrifugation process in the solution containing dichloromethane and ethanol (5:1, v/v).

**Synthesis of the CdSe QDs for comparison in photocatalytic reaction.** The synthesis of CdSe NCs was performed based on classical hot injection methods[1] with a modification. Before the synthesis of the CdSe NCs, precursors were prepared. A clear cadmium oleate ($Cd(oleate)_2$) precursor solution (0.1 M) was obtained by dissolving 3 mmol of CdO in 12 mmol of OAc at 200 °C for more than 6 h under the protection of argon atmosphere, followed by dilution in 25.8 mL degassed ODE. For the TOPSe precursor, TOP solution and Se powder in a molar ratio of 1:1 were mixed and stirred at room temperature overnight in a glovebox, and then diluted in ODE to acquire a concentration of 0.5 M. For the synthesis of QDs 478 and QDs 510, 1 mL of Cd precursor was mixed with 4 mL of ODE, degassed for more than 20 min and stirred under 260 °C for 5 min. 0.2 mL of Se precursor was then quickly injected and

the reaction was kept for 30 s and 10 min for QDs 478 and QDs 510, respectively. For QDs 563, 1 mL of Se precursor was used, and the reaction was kept for 10 min. The purification was performed by adding a solution containing hexane and ethanol (1:1, v/v) and recycling the centrifugation and redispersion process for three times.

**Surface ligand exchange with MPA on the CdSe NCs (both NTs and QDs).** To obtain an aqueous solution of CdSe NTs and QDs, MPA was used to replace the originally hydrophobic ligand on the NCs. First, ethanol was added to the purified CdSe NCs in hexane, followed by a centrifugation to discard the supernatant. The precipitates were well dispersed in 1 mL dichloromethane and 0.2 mL of MPA was added. Then a vortex mixing process of 10 min was applied, after which two centrifugation and redispersion processes were performed in dichloromethane. The mass of NCs was measured after evaporating the dichloromethane. Finally, the NCs were dispersed in deionized water with a concentration of 12.5 mg/mL. The pH value of the solution was adjusted to 9 to get a stable dispersion of the NCs.

**Photocatalytic reduction of the RhB into its leuco form.** Typically, 5 μL of MPA and 12 μL of CdSe NTs was added to a 3 mL RhB water solution (0.05 mg/mL, pH=7). The reaction was triggered by irradiating the visible light from a halogen lamp (HAL 100, Zeiss, 100 W bulb) with an ultra-violet filter (400~2500 nm luminescent spectrum). A stirring speed of 600 rpm was used to improve the mixing during the reaction. After a given time interval, 100 μL of solution was fetched and mixed with 900 μL water for the absorption spectroscopy measurement.

**Characterization.** UV-vis absorption spectroscopy was performed on a Varian Cary 50 Scan UV-vis spectrophotometer. Photoluminescence (PL) and photoluminescence excitation (PLE) spectra were measured by a Horiba fluorescence spectrometer, in which an excitation wavelength was set as 350 nm for the PL spectra and an emission wavelength was set as 600 nm for the PLE spectra. Transmission electron microscopy (TEM) graphs, high-resolution TEM (HRTEM) graphs, selected area electron diffraction (SAED) patterns, scanning transmission electron microscopy (STEM) images and energy-dispersive x-ray spectroscopy (EDX) images were captured by a Talos transmission electron microscope (FEI Co.) and a Titan Themis (FEI Co.); prior

to that, the CdSe NCs dissolved in hexane were dropped and dried on ultrathin carbon-supported copper grids. Scanning electron microscopy (SEM) images were taken on Zeiss Gemini 300 field emission scanning electron microscopes under the in-lens mode operating at an accelerating voltage of 3 kV. Powder X-ray diffraction (XRD) measurement was performed on a Brucker D8 discover X-ray powder diffractometer. Fourier-transform infrared spectroscopy (FTIR) spectra were recorded by a Nicolet iS10 FT-IR Spectrometer (Thermo Scientific) equipped with a smart diamond attenuated total reflectance (ATR) accessory. Thermal gravimetric analysis (TGA) curve was measured by a TGA 4000 from Perkin Elmer.

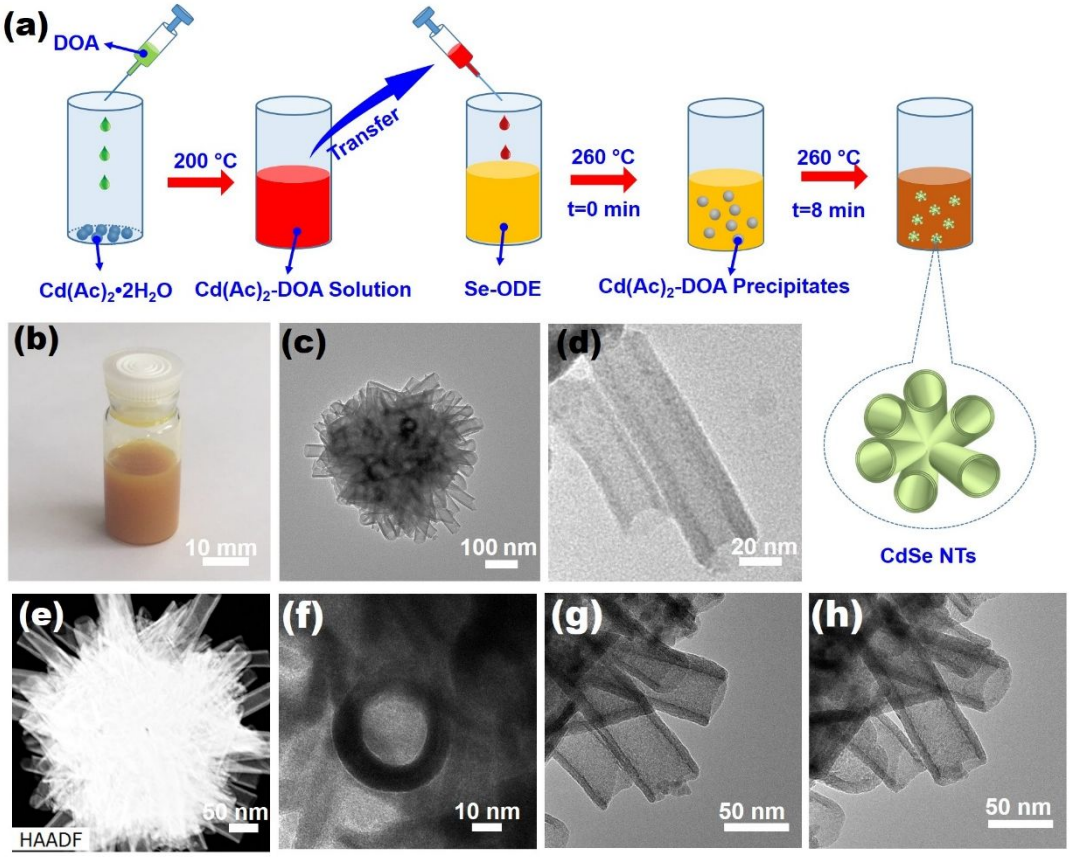


**Figure S1 Synthesis and morphological characterization of the tubular CdSe structures. (a)** Schematic drawing showing the procedures to synthesize the CdSe NTs. Optical image **(b)**, TEM graphs **(c, d)**, STEM graph **(e)** of CdSe NTs synthesized within 8 min at 260 °C. (f) TEM graphs of CdSe NTs showing an intact tube opening **(f)**, as well as NT views after tilting the TEM sample rod for 25 degrees **(g, h)**.

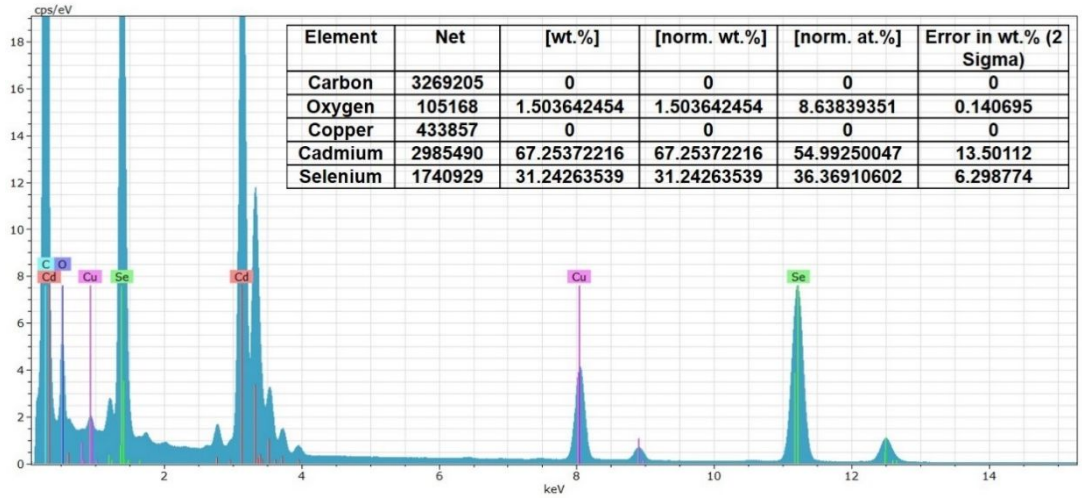


| Element | Net | [wt.%] | [norm. wt.%] | [norm. at.%] | Error in wt.% (2 Sigma) |
|---|---|---|---|---|---|
| Carbon | 3269205 | 0 | 0 | 0 | 0 |
| Oxygen | 105168 | 1.503642454 | 1.503642454 | 8.63839351 | 0.140695 |
| Copper | 433857 | 0 | 0 | 0 | 0 |
| Cadmium | 2985490 | 67.25372216 | 67.25372216 | 54.99250047 | 13.50112 |
| Selenium | 1740929 | 31.24263539 | 31.24263539 | 36.36910602 | 6.298774 |

**Figure S2 EDX spectra and semi-quantitative analysis of the elements in the CdSe NTs.** EDX analysis of the CdSe NTs synthesized during 8 min, which shows the presence of Cd, Se, O, C and Cu. The table on the top right shows the semi-quantitative analysis among Cd, Se and O elements.

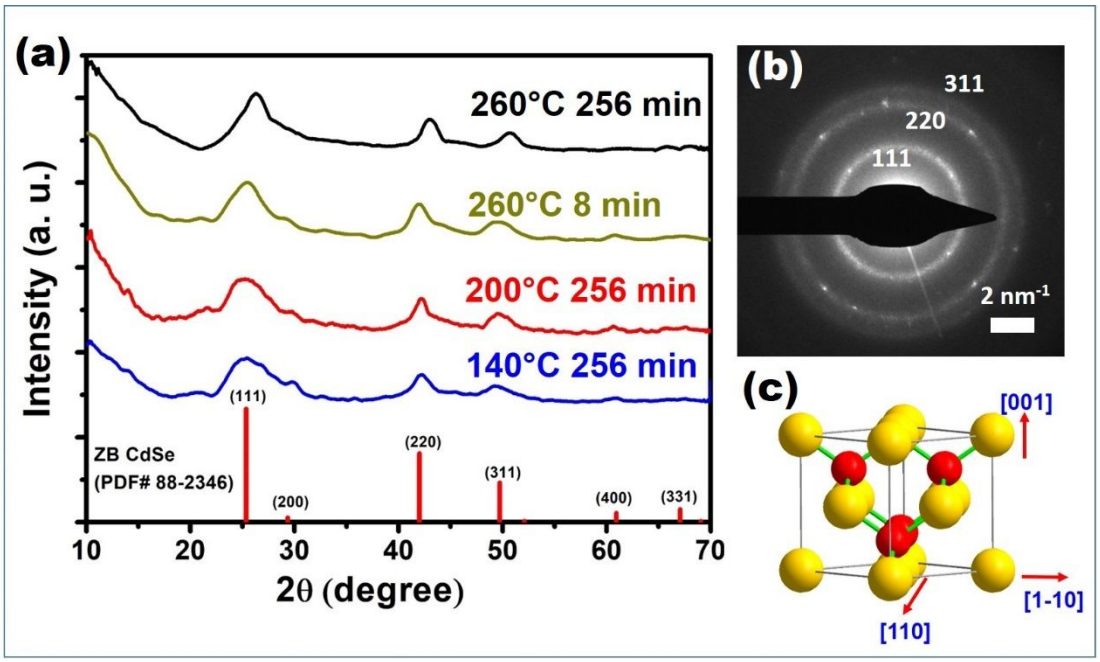


**Figure S3 Crystallographic structure characterization of the 2D CdSe NCs. (a)** XRD pattern of the 2D CdSe NCs synthesized at different conditions, including at140 °C for 256 min (blue), at 200 °C for 256 min (red), at 260 °C for 8 min (yellow-green) and at 260 °C for 256 min (black), from the bottom to top. Vertical lines on the bottom represent the standard XRD pattern of bulk zinc-blende CdSe (PDF no. 88-2346). **(b)** SAED pattern of the 2D CdSe NTs synthesized within 8 min at 260 °C. **(c)** A schematic illustration of a unit cell of the zinc-blende CdSe crystal.

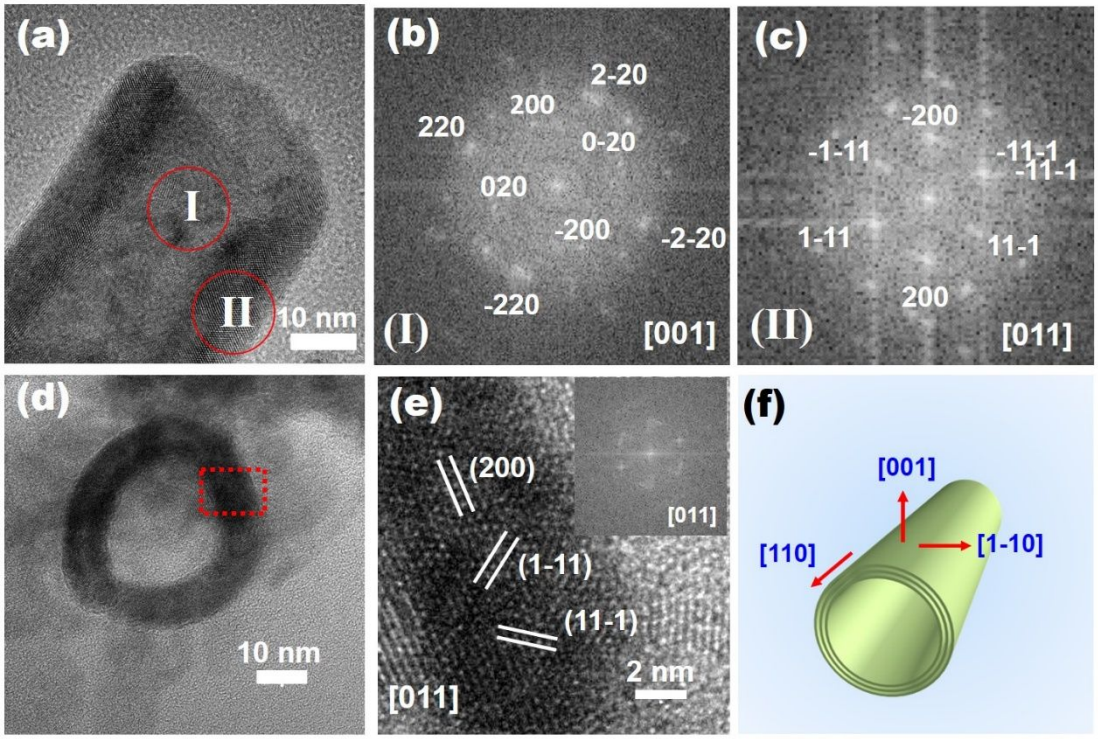


**Figure S4 HRTEM characterization of the growth orientations in CdSe NTs. (a)** HRTEM graph of a CdSe NT, with fast Fourier transform (FFT) pattern of **(b)** the center (location of area I in a), showing 4-fold rotational symmetry of a face-centered cubic (fcc) structure, as observed along the [001] zone axis, and of **(c)** the edge (location of area II in a), showing the characteristic pattern of a fcc structure, as observed along the [011] zone axis. **(d)** HRTEM graph of a CdSe NT, as observed normal to the tube opening, showing lattice spacings corresponding to the {200} and {111} planes of fcc CdSe. **(e)** Zoom on the rectangle in (d), the FFT pattern of the inset indicates that the observation zone axis is [011]. **(f)** Schematic illustration showing that the lateral, angular and thickness growth directions in the CdSe NT are [110], [1-10] and [001], respectively.

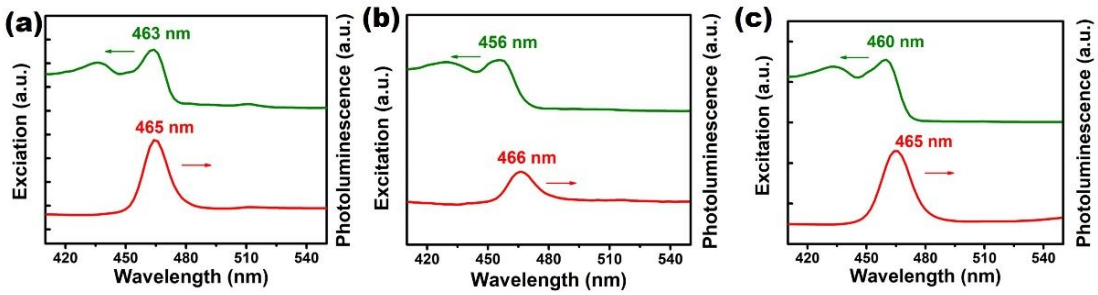


**Figure S5 Photoluminescence excitation (PLE, green) and photoluminescence (PL, red) spectra of a CdSe NTs in hexane solution.** The samples were synthesized from Cd acetate-dioctylamine ($Cd(Ac)_2$-DOA) and Se-octadecene (Se-ODE) precursor solutions at 260 ºC during a reaction time of (a) 8 min, (b) 256 min, and (c) 8 min, with additional exchange of acetate ligands by oleic acid (OAc) at 200 °C for10 min.

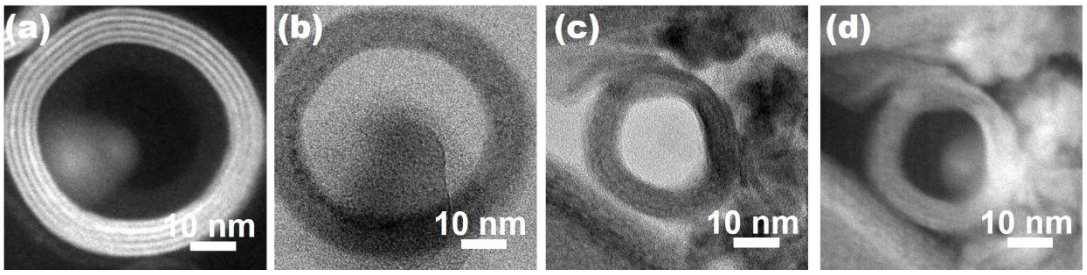


**Figure S6 High-magnification (a, d) STEM and (b, c) TEM images of CdSe NTs observed along the tube-opening direction.** (a, d) High-magnification STEM and (b, c) TEM images of nanotubes synthesized within 8 min observed along the tube opening direction. If we first imaged the nanotube under STEM mode, clear features on an individual-wall scale can be observed (a), which became blurred once we turned to TEM mode (b). Instead, if the TEM graphs were taken first (c), we found it was later more difficult to visualize clearly individual walls in the STEM mode too (d).

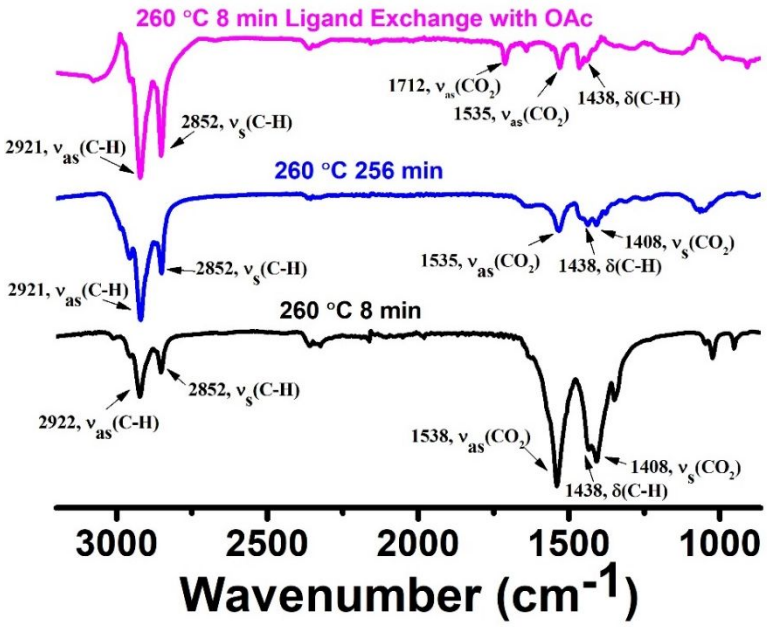


**Figure S7 FTIR spectra of CdSe NCs synthesized at different conditions.** FTIR spectra of CdSe NCs synthesized at 260 °C for 8 min (black), for 256 min (blue) and for 8 min followed by a further ligand exchange with OAc (pink). For samples synthesized at 260 °C for 8 min, the dominant peaks at 1538 and 1408 $cm^{-1}$ are assigned to the antisymmetric and symmetric stretching vibration mode of COO- in the acetate group, respectively. For samples synthesized at 260 °C for 256 min, the major peaks are at 2921 and 2852 $cm^{-1}$, corresponding to the antisymmetric and symmetric stretching vibration mode of C-H, indicative of presence of a large quantity of DOA. For samples synthesized at 260 °C for 8 min with a further ligand exchange with OAc, a characteristic peak at 1712 $cm^{-1}$ related to the antisymmetric stretching vibration mode of COO- in oleate is present.

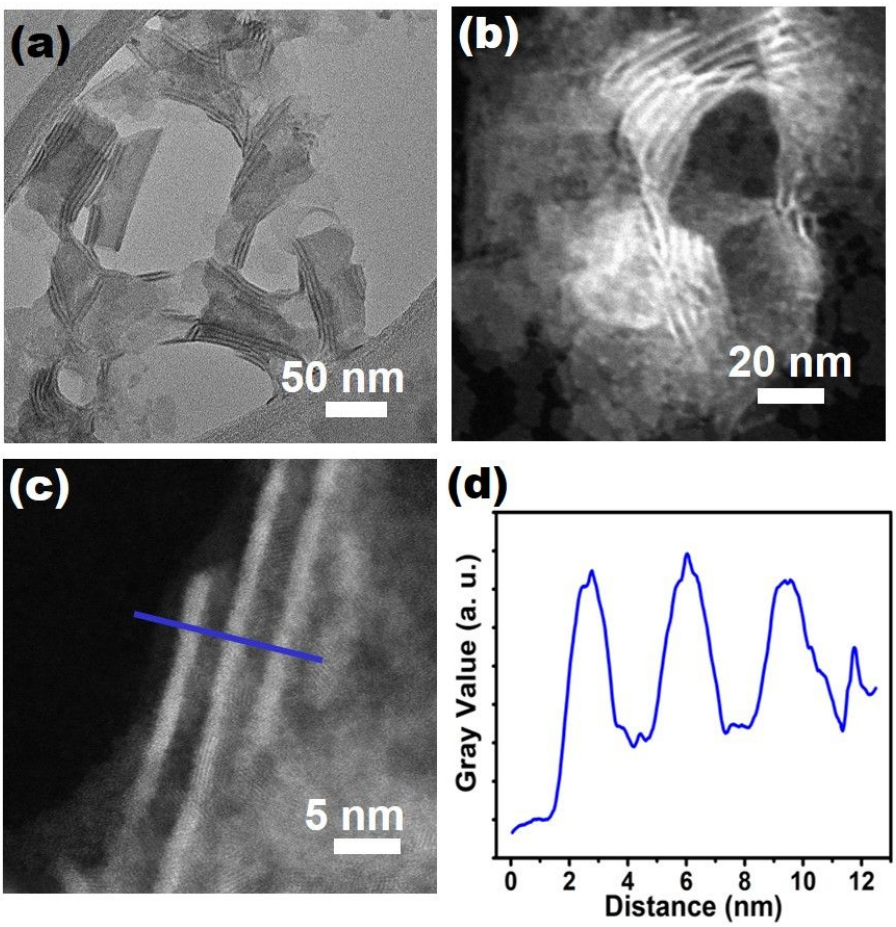


**Figure S8 TEM and STEM graphs of the CdSe NTs after ligand exchange with oleic acid. (a)** TEM and **(b, c)** STEM graphs showing **(a, b)** an overview and **(c)** a close-up of the CdSe NTs synthesized at 260 °C for 8 min followed by a further ligand exchange with OAc. **(d)** Profile analysis of the thickness based on the gray contrast in (c).

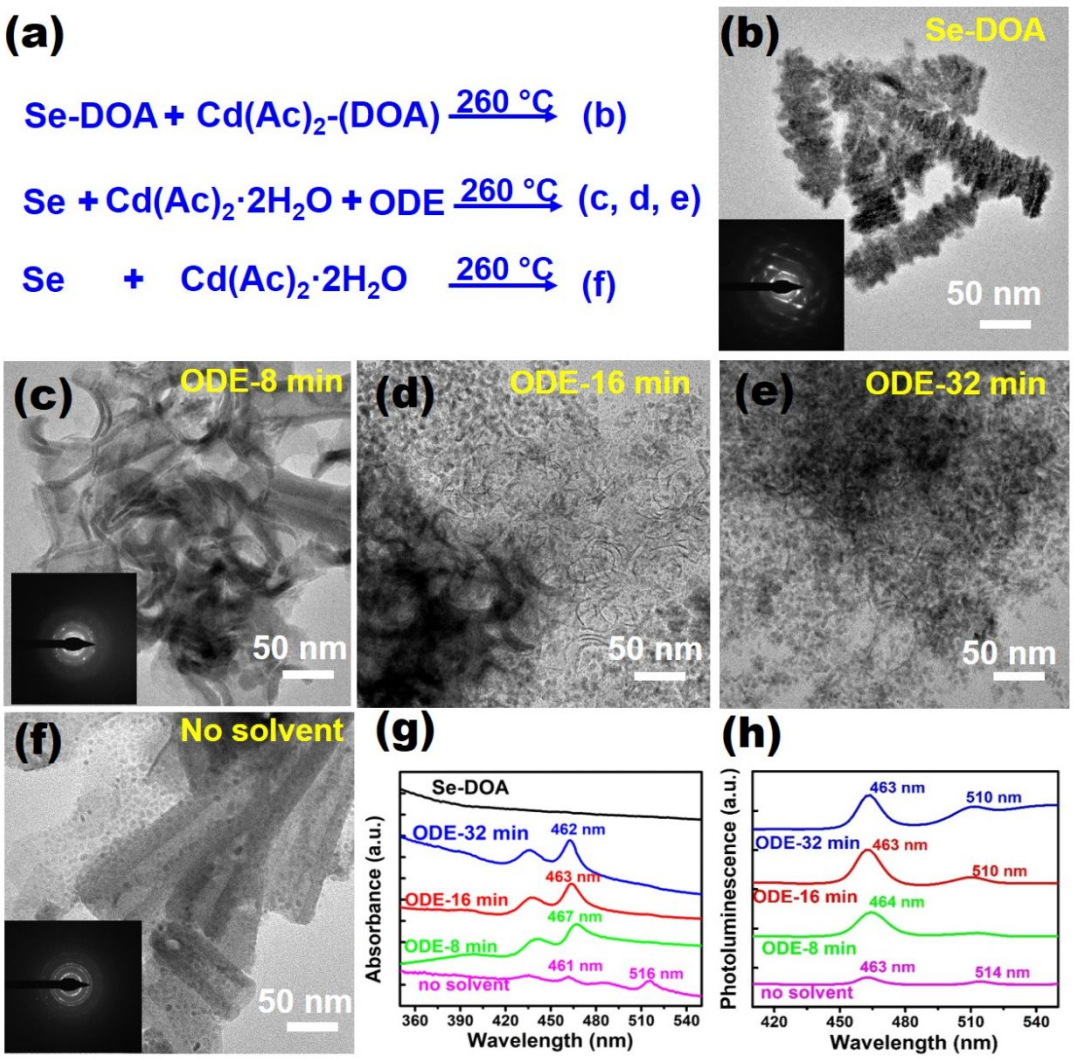


**Figure S9 Control experiments to study the role of acetate and amine ligand in the synthesis of 2D CdSe NCs. (a)** Formulas describing the design of control experiments to investigate the role of acetate and amine in the CdSe NT formation. **(b)** TEM graph of large-size CdSe mesocrystals assembled from quantum dots, which were synthesized by using $Cd(Ac)_2$-DOA and Se-DOA as precursors at 260 °C for 8 min. The SAED pattern in the inset of (b) indicates the characteristic mesocrystal structure, as observed along [011] zone axis. **(c-e)** TEM graphs of CdSe NCs synthesized by reacting the mixture of Se and $Cd(Ac)_2 \cdot 2H_2O$ in ODE solvent at 260 °C for 8 min (c), 16 min(d) and 32 min (e). The SAED pattern in the inset of (c) indicates the characteristic CdSe NCs pattern of a tube-like structure. **(f)** TEM graph of CdSe NCs synthesized by reacting the mixture of Se and $Cd(Ac)_2 \cdot 2H_2O$ without solvent at 260 °C for 8 min. The SAED pattern in the inset shows the characteristic CdSe NCs pattern rather than the Cd precursor pattern. **(g)** UV-vis absorbance and **(h)** PL spectra of the samples as shown in (b-f), which were labelled as Se-DOA (black curve, sample in b), ODE-32 min (blue curve, sample in c), ODE-16 min (red curve, sample in d), ODE-8 min (green curve, sample in e) and no solvent (blue curve, sample in f), respectively.

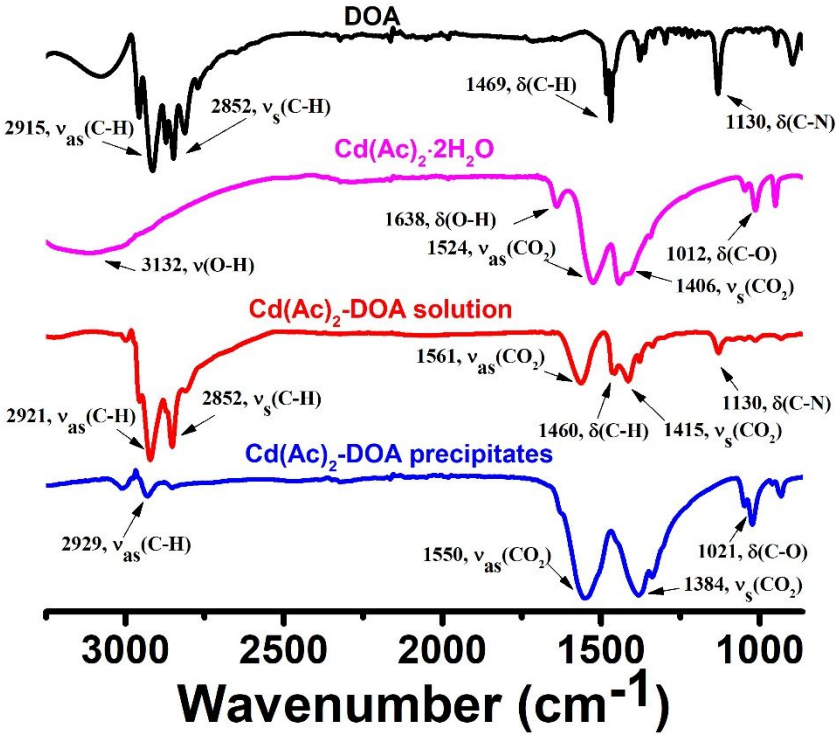


**Figure S10 FTIR spectra of DOA, $Cd(Ac)_2 \cdot 2H_2O$, $Cd(Ac)_2$-DOA solution and $Cd(Ac)_2$-DOA precipitates.** FTIR spectra of DOA with characteristic peaks at 2915, 2852, 1469, and 1130 $cm^{-1}$ (black), of $Cd(Ac)_2 \cdot 2H_2O$ (pink), of $Cd(Ac)_2$-DOA solution (red) and of $Cd(Ac)_2$-DOA precipitates (blue). For DOA, characteristic peaks at 2915, 2852, 1469 $cm^{-1}$ are assigned to the vibration of C-H, and the peak at 1130 $cm^{-1}$ relate to the bending vibration of the C-N bond. For $Cd(Ac)_2 \cdot 2H_2O$, the major peaks are at 1524 and 1406 $cm^{-1}$, corresponding to the antisymmetric and symmetric stretching vibration mode of COO- in the acetate group. The difference in wavenumber between the two peaks is 118 $cm^{-1}$, indicating the role of acetate in coordinating to the Cd center is a chelating and bridging interaction[3,4]. For the $Cd(Ac)_2$-DOA solution, the spectra shows both features of the acetate group and DOA, especially with the clear peak at 1130 $cm^{-1}$ corresponding to the bending vibration of C-N bond in DOA. For $Cd(Ac)_2$-DOA precipitates, the spectra is almost similar to that of $Cd(Ac)_2 \cdot 2H_2O$, with an increase of the difference in wavenumber between the antisymmetric and symmetric stretching vibration of COO- in the acetate group (166 $cm^{-1}$) that can be explained by the loss of the hydrate water.

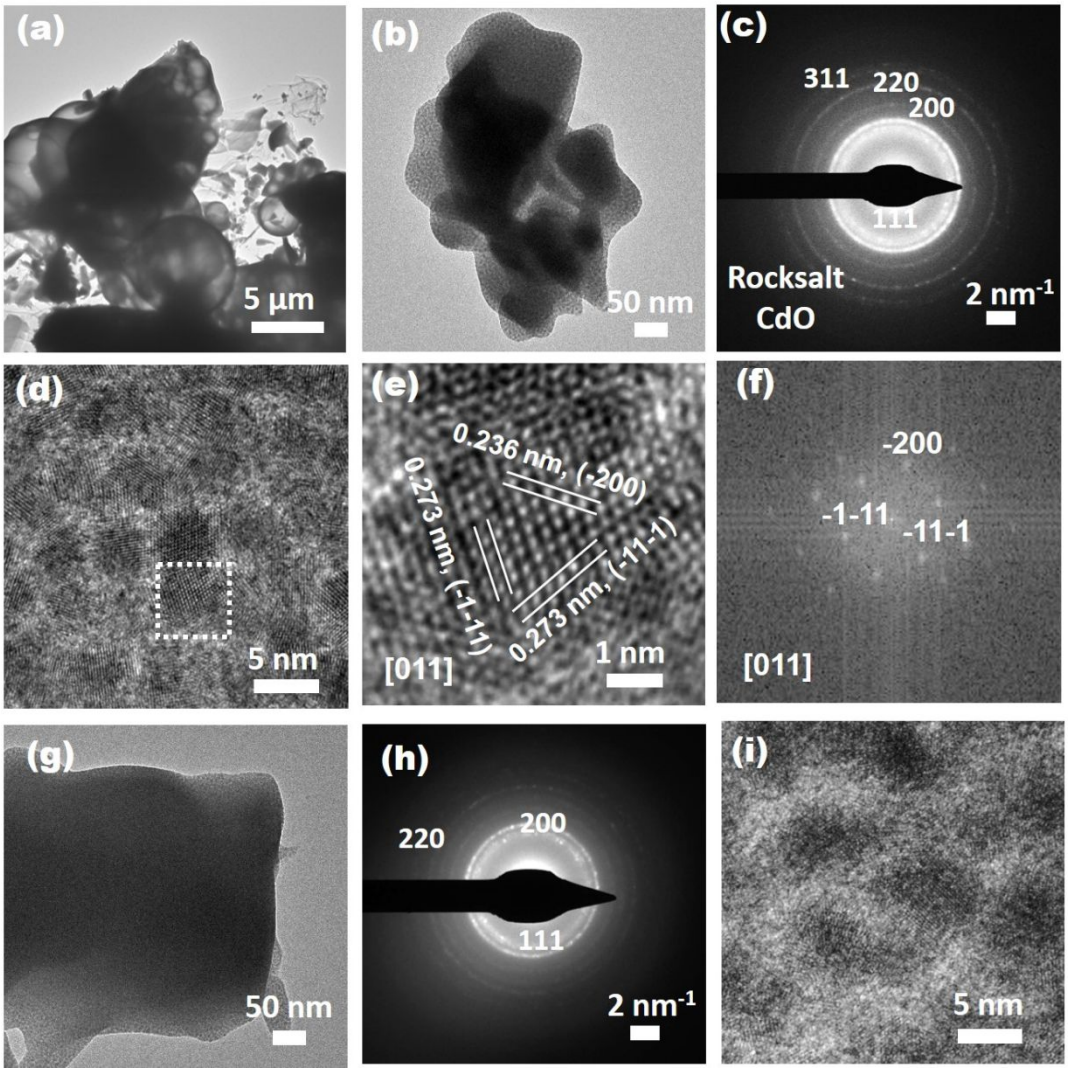


**Figure S11 Morphological and structural characterization of $Cd(Ac)_2 \cdot 2H_2O$ powders and $Cd(Ac)_2$-DOA Precipitates by TEM. (a,c)** TEM graphs, **(b)** SAED pattern and **(d,e)** HRTEM graphs of the $Cd(Ac)_2 \cdot 2H_2O$ powder observed under an accelerating voltage of 200 kV. Rapid observation of the large-size crystals under low magnification shows the phase transition of the $Cd(Ac)_2 \cdot 2H_2O$ crystals under electron beam radiation (a). An amorphous matrix with distributed CdO NCs of 3~6 nm was found under high-magnification observation (b). The SAED pattern well matches with the low-index planes in rock-salt (fcc) structure (PDF no. 75-0593). The lattice fringes spacing of 0.273 nm and 0.236 nm in the NCs are corresponding to the {111} planes and {200} planes in bulk CdO NCs, which was verified by **(f)** the FFT analysis showing the characteristic pattern as observed along [011] zone axis. Formation of CdO NCs is attributed to the transformation of amorphous $Cd(Ac)_2 \cdot 2H_2O$ under electron beam radiation. **(g)** TEM graph, **(h)** SAED pattern and **(i)** HRTEM graph of the $Cd(Ac)_2$-DOA precipitate. Except the emergence of larger CdO NCs of 5~8 nm, the morphology and crystal structure of a $Cd(Ac)_2$-DOA precipitate are almost the same as that of $Cd(Ac)_2 \cdot 2H_2O$ powder.

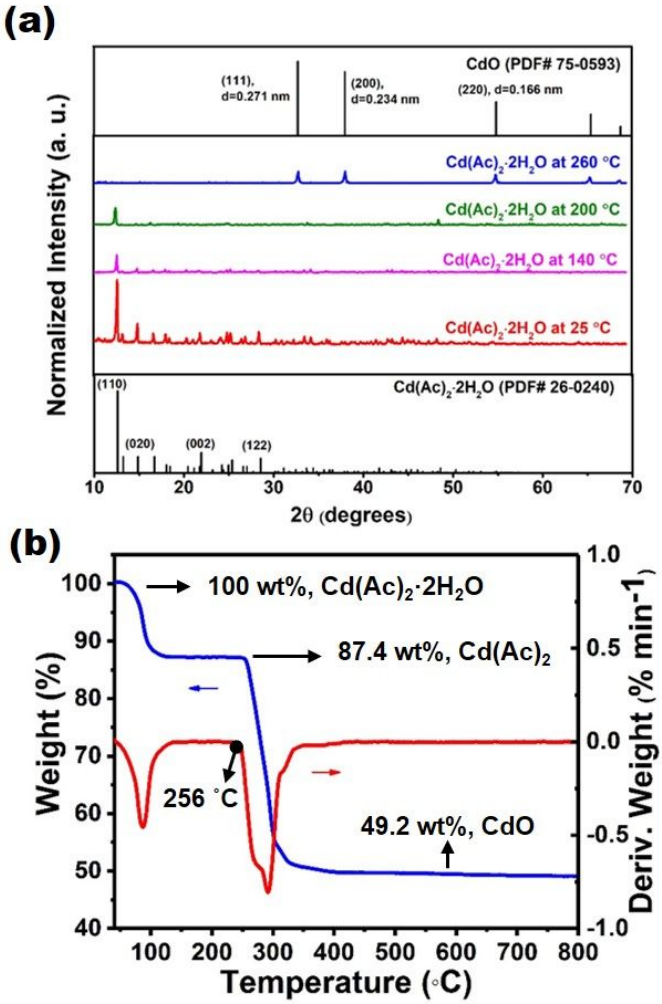


**Figure S12 Structural characterization of $Cd(Ac)_2{\cdot}2H_2O$ powders treated at different temperatures.** (a) XRD pattern of $Cd(Ac)_2{\cdot}2H_2O$ powders treated at different temperatures, including 25 °C (red, no treatment), 140 °C (pink), 200 °C (green) and 260 °C (blue). The treatment was conducted by heating $Cd(Ac)_2{\cdot}2H_2O$ powders at the given temperature for 30 min, followed by cooling in air. A strong and clear signal of $Cd(Ac)_2{\cdot}2H_2O$ crystals was found without treatment (25 °C), while the intensity sharply decreased at 140 °C (pink) and 200 °C (green), indicating more and more crystals turned into an amorphous structure after heating. When the sample was treated at 260 °C, only the characteristic signal of CdO crystals was observed, demonstrating the transformation of $Cd(Ac)_2{\cdot}2H_2O$ into CdO crystals. Vertical lines on the top and bottom represent the standard XRD patterns of CdO crystal (PDF no. 75-0593) and $Cd(Ac)_2{\cdot}2H_2O$ (PDF no. 26-0240), respectively. (b) Thermal gravimetric analysis (TGA, blue) curve and the corresponding differential curve (DTG, red) of $Cd(Ac)_2{\cdot}2H_2O$ powders from 35 ˚C to 800 ˚C under nitrogen atmosphere. These curves show the $Cd(Ac)_2{\cdot}2H_2O$ powders would start to lose crystal water above 35 ˚C, possible reason for the transformation from crystal to amorphous structure. Then from 256 ˚C, it starts to decompose to crystallized CdO.

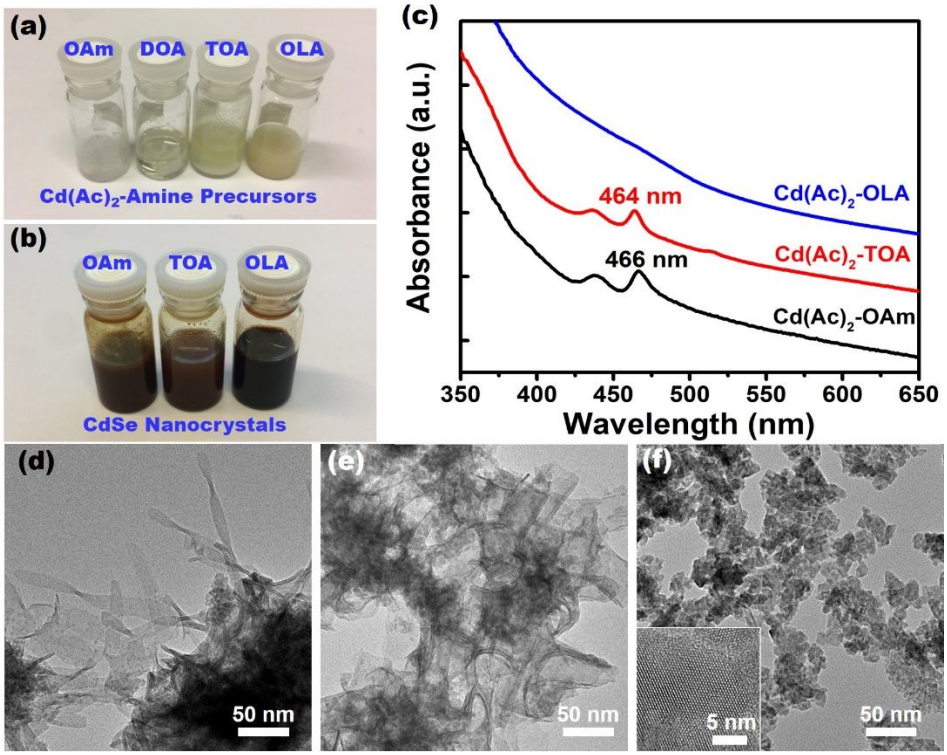


**Figure S13 Influence of primary and tertiary alkylamines on the morphology of the CdSe NCs.** (a) Photograph of the $Cd(Ac)_2$-amine precursor solutions prepared by different alkylamines, including octylamine (OAm), dioctylamine (DOA), trioctylamine (TOA), and oleylamine (OLA). $Cd(Ac)_2$ is well dissolved in OAm, DOA and OLA, once heated, while it can only form a turbid suspension in TOA due to the steric effect. In particular, clear $Cd(Ac)_2$-OAm and $Cd(Ac)_2$-OLA solutions would be solids at room temperature. (b) Photograph, (c) UV-Vis absorption and (d-f) TEM graphs of the CdSe nanocrystals synthesized at 260 ° C for 8 min using different Cd precursors, including (d) $Cd(Ac)_2$-OAm, (e) $Cd(Ac)_2$-TOA and (f) $Cd(Ac)_2$-OLA. The inset in (f) indicates the high crysatllininty of the CdSe nanoparticle aggreagates.

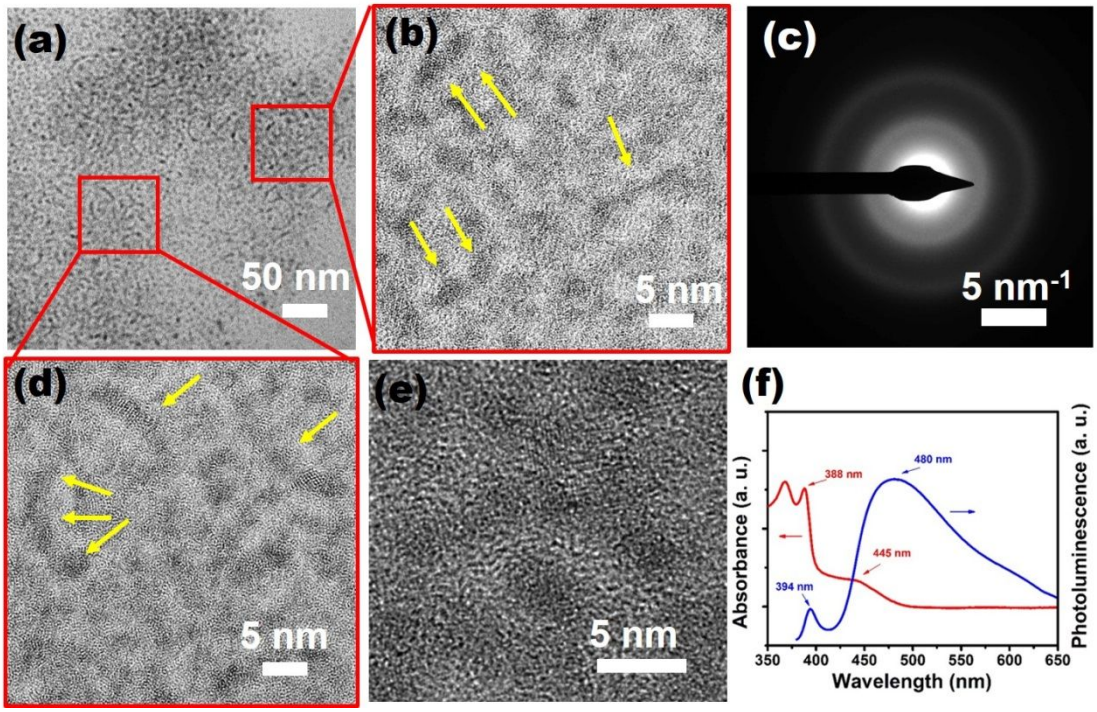


**Figure S14 Characterization of 2D CdSe NCs synthesized at 80 °C for 17 hours.** **(a,b,d,e)** TEM graphs, **(c)** SAED pattern, **(f)** UV-vis absorption and PL spectra of the 2D CdSe NCs synthesized at 80 °C for 17 hours. The graphs show the assembly of the nanoscale platelet-like structures of around 2 nm in thickness of (e) by a lateral (b) and angular (d) attachment mechanism. The SAED pattern of (c) indicates these NCs, synthesized at low temperature, have zinc-blende structure with relatively undeveloped crystallinity. The spectroscopic data of (f) exhibit the characteristic absorption and emission peak of 2D CdSe NCs at around 390 nm. The very broad PL peak at around 480 nm is ascribed to the deep trap emission in the 2D CdSe NCs. The absorption at 455 nm in the absorption spectra could be assigned to unpurified quantum dots of around 2 nm.

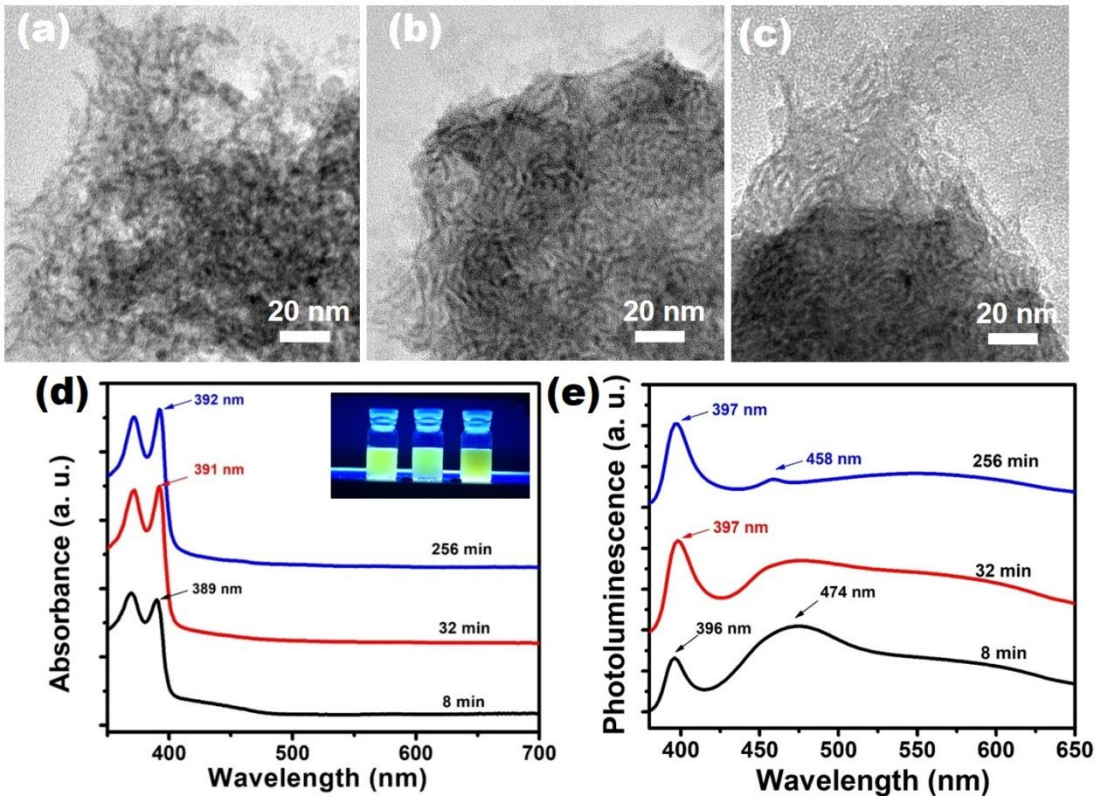


**Figure S15 Characterization of 2D CdSe NCs synthesized at 140 °C for 8, 32 and 256 minutes. (a-c)** TEM graphs, **(d)** UV-vis absorption, and **(e)** PL spectra of the 2D CdSe NCs synthesized at 140 °C for 8 (a), 32 (b) and 256 (c) min. The small redshift of the first excitonic peak from 389 to 392 nm in (d) is ascribed to the growth of the 2D NCs in the lateral or angular direction. Consistently, the broad PL peak at around 474 nm in (e) gradually reduces with increasing reaction time because of crystal growth.

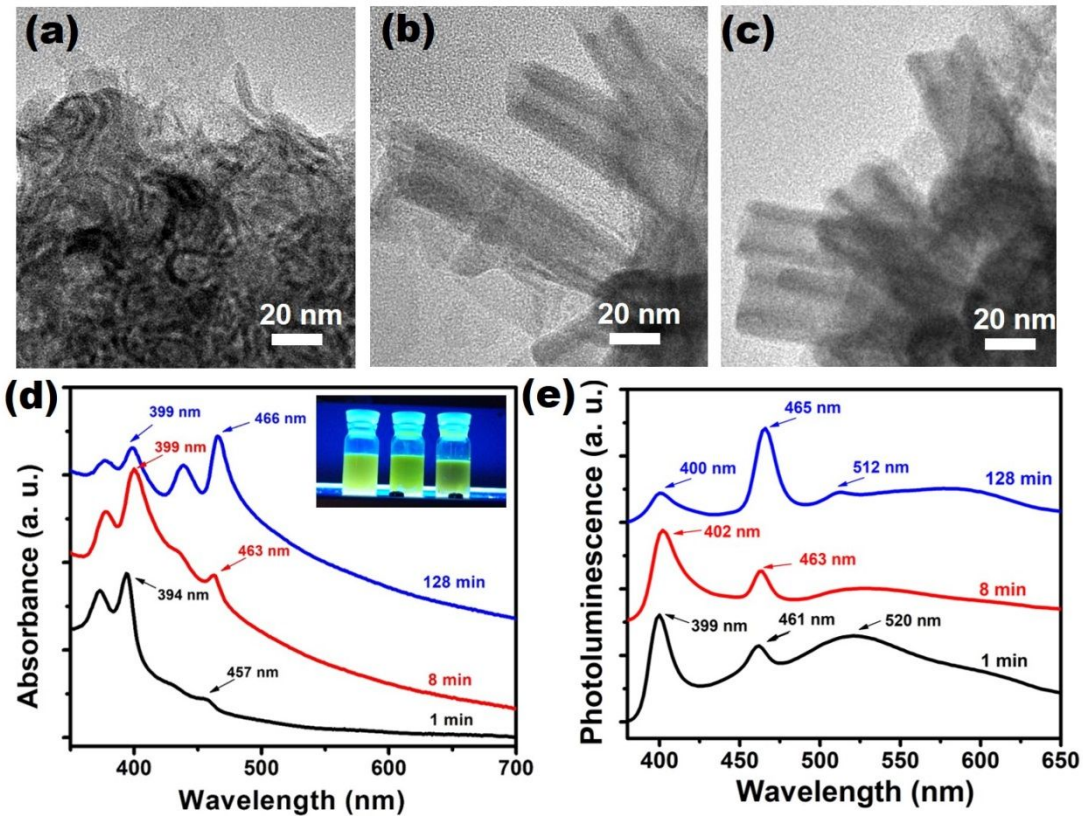


**Figure S16 Characterization of 2D CdSe NCs synthesized at 200 °C for 1, 8 and 128 minutes. (a-c)** TEM graphs, **(d)** UV-vis absorption and **(e)** PL spectra of the 2D CdSe NCs synthesized at 200 °C for 1 (a), 8 (b) and 128 (c) min. The redshift of the major excitonic peak from 394 to 399 nm as well as from 457 to 466 nm in (d) is ascribed to the growth of the 2D NCs. Consistently, growth of the 2D NCs results in the decrease of the broad PL peak at around 520 nm in (e) due to the deep trap emission, as well as the increase of the sharp PL peak at around 465 nm, as more 2D NCs with thickness of 6.5 MLs were formed.

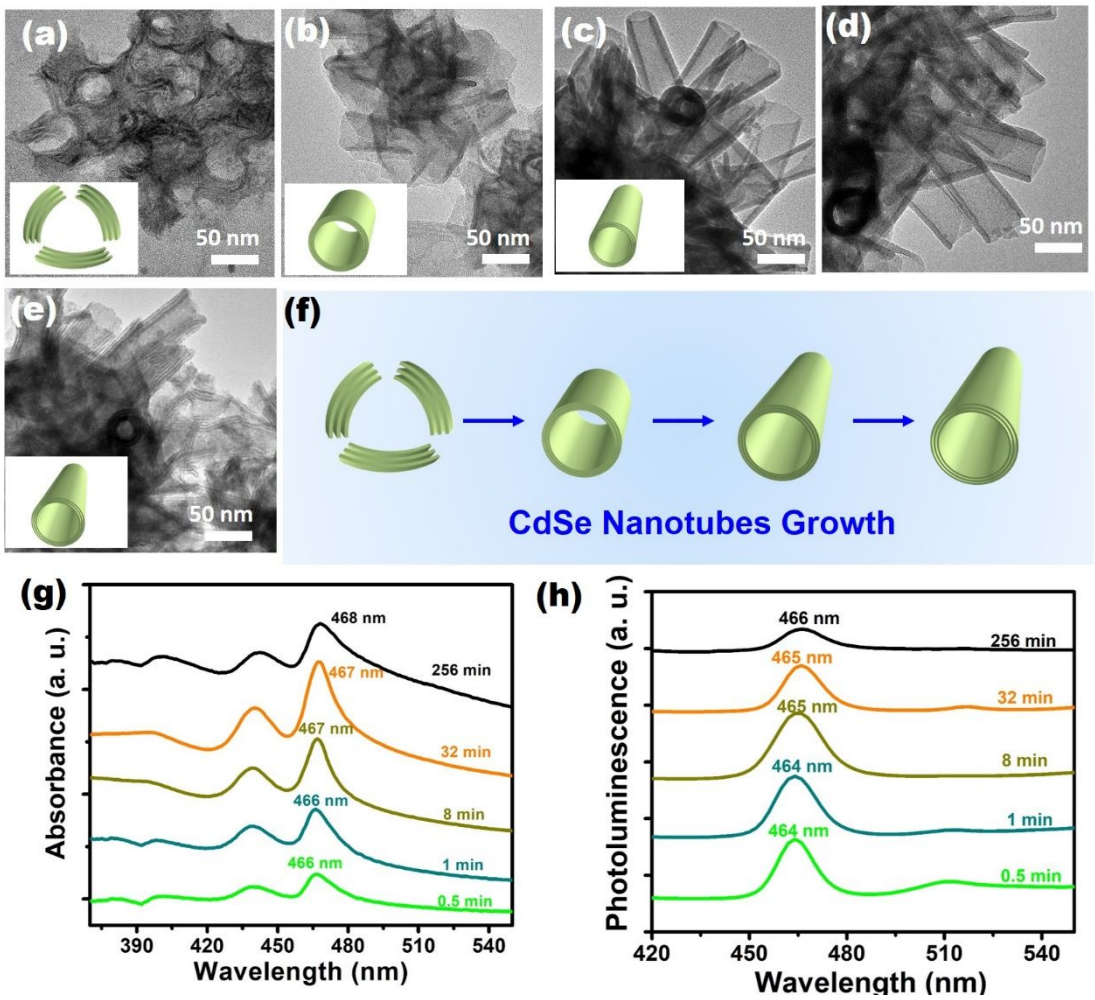


**Figure S17 Characterization of 2D CdSe NCs synthesized at 260 °C for 0.5, 1, 8, 32 and 256 minutes. (a-e)** TEM graphs, **(g)** UV-vis absorption, and **(h)** PL spectra of the 2D CdSe NCs synthesized at 260 °C for 0.5 (a), 1 (b), 8 (c), 32 (d) and 256 (e) and 128 (f) min. The small redshift of the first excitonic peak from 466 to 468 nm in (g) and of the PL peak from 464 to 466 nm in (h) are ascribed to the growth of the 2D NCs. **(f)** Schematic drawing of the assembly of the curved nanosheets into well-defined tubular structures that finally turn into NTs with visible multiple walls.

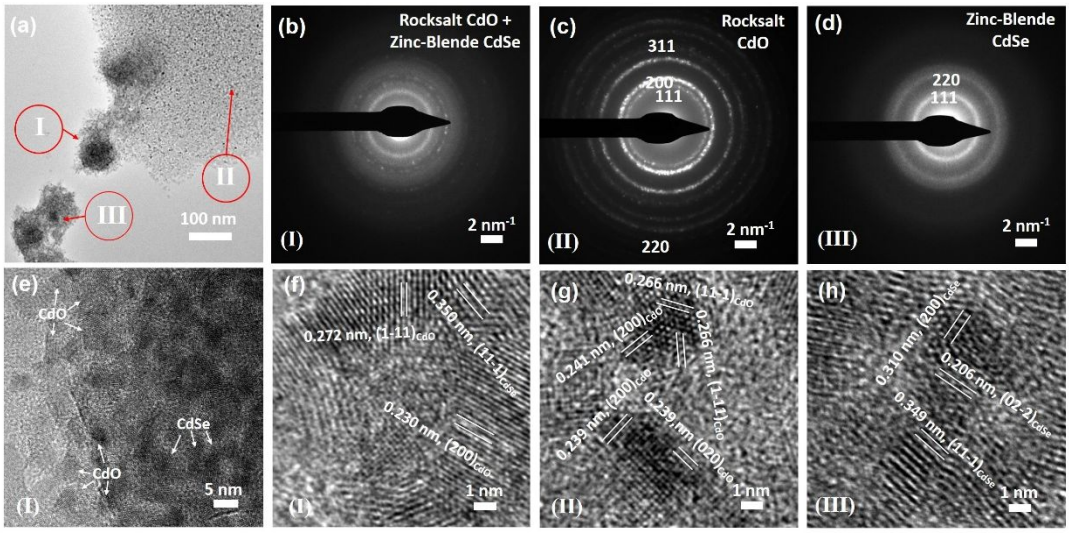


**Figure S18 TEM characterization of early stage formation of the 2D CdSe NCs from Cd precursor matrix. (a)** TEM graph, **(b-d)** SAED patterns, and **(e-h)** HRTEM graphs showing the early growth stage of the 2D CdSe NCs obtained from the samples prepared at 140 °C for 8 min. CdO NCs can be eventually generated from unreacted Cd precursor under electron beam radiation. Region I in (a) shows the coexistence of rocksalt CdO NCs and zinc-blende CdSe NCs (b,e,f), indicating the formation 2D CdSe NCs from solid Cd precursor matrix. Region II and III in (a) display the unreacted Cd precursor matrix filled with CdO NCs (c,g) and aggregates of 2D CdSe NCs (d, h).

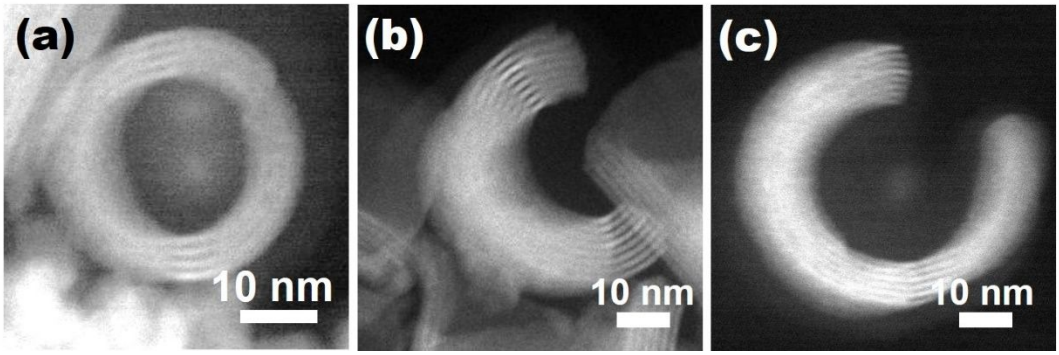


**Figure S19 Final and incomplete formation of CdSe NTs observed along the tube opening direction.** TEM graphs of CdSe NTs synthesized at 260 °C for a reaction time of 8 min, showing the (a) intact and (b,c) incomplete assembly of curved multi-layered nanosheets into NTs.

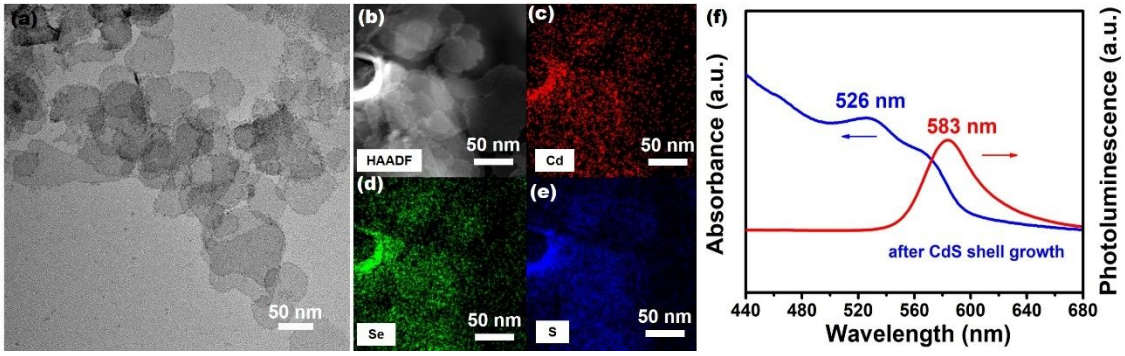


**Figure S20 Characterization of nanostructures after growing a CdS shell on the CdSe NTs.** (a) TEM, (b) HAADF-STEM, EDX mapping of (c) Cd, (d) Se and (e) S, (f) UV-Vis and photoluminescence of the nanostructures after growing a CdS shell on the CdSe nanotubes. The reaction was performed by reacting CdSe nanotubes with thioacetamide (TTA), followed by the addition of $Cd(OA)_2$.

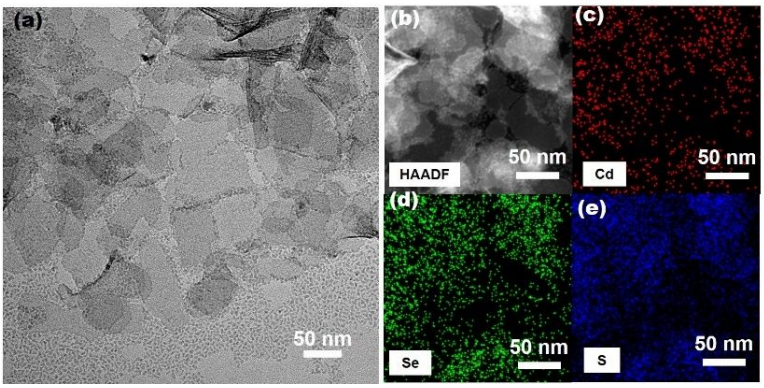


**Figure S21 Characterization of nanostructures after reacting CdSe NTs with thioacetamide.** (a) TEM, (b) HAADF-STEM, EDS mapping of (c) Cd, (d) Se and (e) S of the nanostructures after reacting CdSe nanotubes with thioacetamide (TTA), i.e. after ligand exchange rather than after growing a CdS shell.

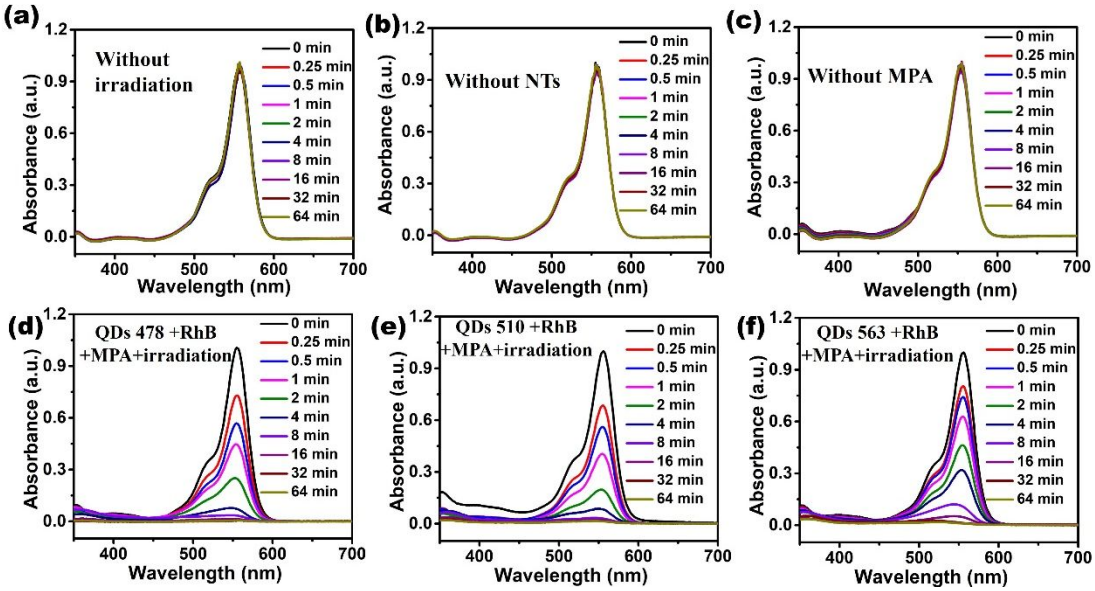


**Figure S22 Temporal evolution of the absorption spectra of the RhB solution under different photoreaction conditions.** A standard photoreduction of RhB was performed by adding the CdSe NTs and MPA into the RhB solution, followed by triggering the light irradiation (beginning of the reaction, named as "0 min"). For comparison, no light irradiation was performed in (a); no CdSe NTs was added in (b); no MPA was added in (c); QDs 478 was used to replace CdSe NTs in (d); QDs 510 was used to replace CdSe NTs in (e); QDs 563 was used to replace CdSe NTs in (f).

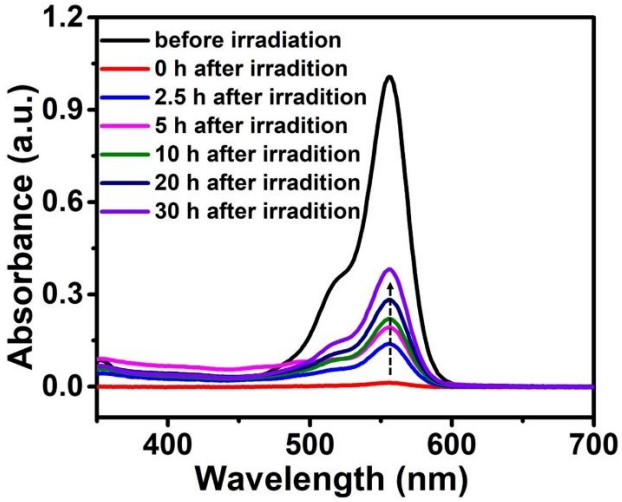


**Figure S23 Absorption spectra showing the self-recovery of leuco RhB into its normal form by exposure during different times to ambient oxygen.** The photoreduction of the RhB was conducted at an irradiation time of 2 min in the presence of CdSe NTs and MPA, this condition corresponding to the curve labeled as '0 h after irradiation'.

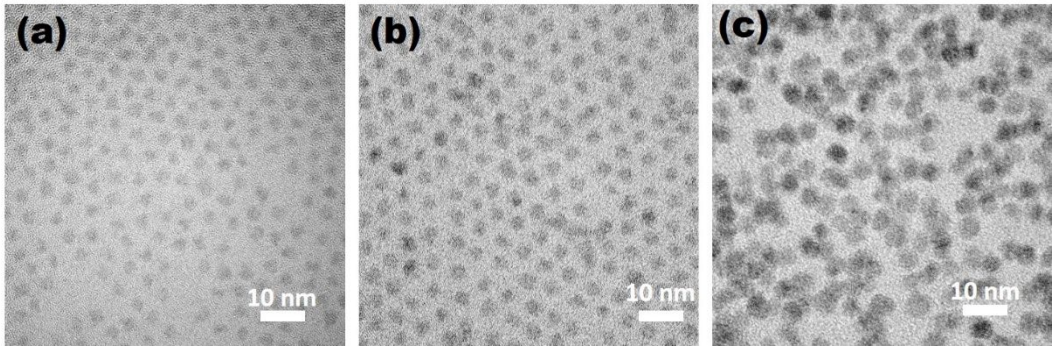


**Figure S24 TEM characterization of CdSe QDs that were used in the comparative study of the photoreduction reaction.** TEM graphs of (a) CdSe QDs 476, (b) QDs 510, and (c) QDs 563.

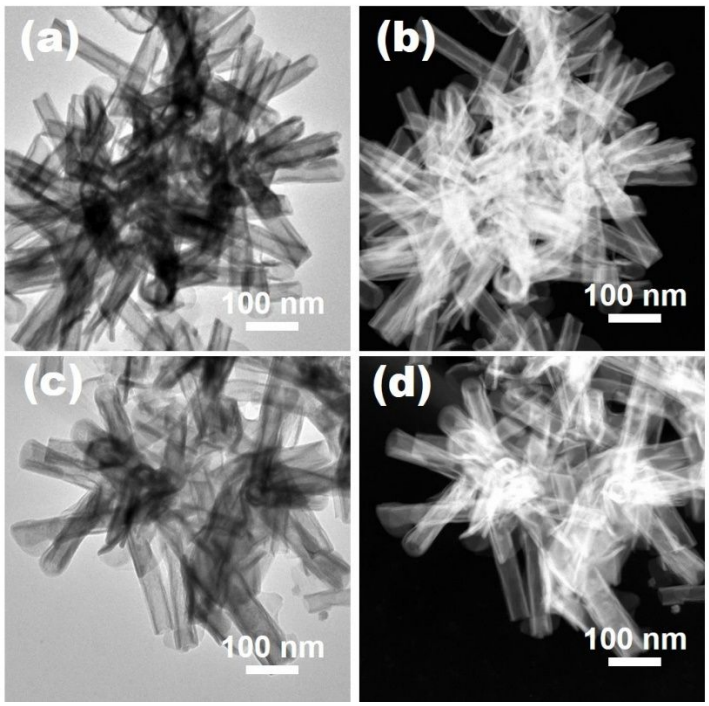


**Figure S25. (a, c) TEM and (b, d) STEM graphs of CdSe NTs before (a,b) and after (c,d) the photocatalytic reaction.** The nanostructures in (a,b) were obtained after the ligand exchange with MPA and dispersed in an aqueous solution with pH value of 9. The photocatalytic reaction was performed during 30 min.

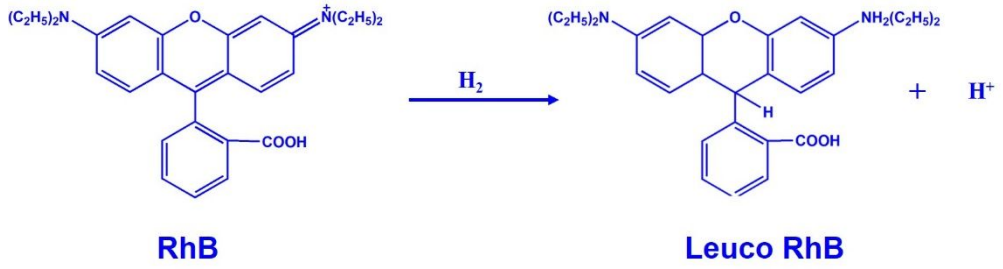


RhB Leuco RhB

**Scheme S1 Reduction of RhB into its leuco form when reacted with hydrogen.**

## References:


1. Peng, Z. A. Peng X. Formation of high-quality CdTe, CdSe, and CdS nanocrystals using CdO as precursor. *J. Am. Chem. Soc.***2001***, 123*, 183-184
2. Mahler, B.; Nadal, B.; Bouet, C.; Patriarche, G.; Dubertret, B. Core/shell colloidal semiconductor nanoplatelets. *J. Am. Chem. Soc.* **2012**, *134* (45), 18591–18598.
3. Deacon, G.; Phillips, R. Relationships between the carbon-oxygen stretching frequencies of carboxylato complexes and the type of carboxylate coordination. *Coord. Chem. Rev.* **1980**, *33*, 227-250.
4. Harrison, W.; Trotter, J. Crystal and molecular structure of cadmium diacetate dihydrate. *J. Chem. Soc., Dalton Trans.* **1972**, *0*, 956-960.